REPORT NO.
UCB/SESM-82/05

STRUCTURAL ENGINEERING AND
STRUCTURAL MECHANICS

FORMULATION AND NUMERICAL INTEGRATION OF ELASTOPLASTIC AND ELASTO-VISCOPLASTIC RATE CONSTITUTIVE EQUATIONS

by

PETER M. PINSKY

KARL S. PISTER

and

ROBERT L. TAYLOR

AUGUST 1982

DEPARTMENT OF CIVIL ENGINEERING
UNIVERSITY OF CALIFORNIA
BERKELEY, CALIFORNIA

Structural Engineering and Structural Mechanics Division
Report NO. UCB/SESM-82/05

FORMULATION AND NUMERICAL INTEGRATION OF ELASTOPLASTIC AND ELASTO-VISCOPLASTIC RATE CONSTITUTIVE EQUATIONS

by

Peter M. Pinsky
Karl S. Pister
and
Robert L. Taylor

Department of Civil Engineering
University of California
Berkeley, California 94720

August 1982

FORMULATION AND NUMERICAL INTEGRATION OF ELASTOPLASTIC AND ELASTO-VISCOPLASTIC RATE CONSTITUTIVE EQUATIONS

Peter M. Pinsky

Division of Engineering
Brown University

Karl S. Pister and Robert L. Taylor

Department of Civil Engineering
University of California, Berkeley

ABSTRACT

Spatial rate constitutive equations for elastoplastic and elasto-viscoplastic materials are considered within a thermodynamic framework in which irreversible processes are characterized through the use of internal state variables and in which no restrictions on the magnitude of the deformation are imposed. The development employs an invariance principle which leads to a unique definition of the objective rate appearing in the rate constitutive equations. The elastic-plastic split of the deformation is introduced through a thermodynamic argument which leads to the additive decomposition of the spatial rate of deformation tensor. Following the development of the rate constitutive equations, a numerical algorithm is presented for their numerical integration. By employing product formula techniques, the proposed algorithm exploits the "operator split" of the spatial rate constitutive equations resulting from the additive decomposition of the rate of deformation tensor. The resulting algorithm is demonstrated to be unconditionally stable and incrementally objective. Finally, an efficient and very accurate implicit global algorithm for the numerical solution of the initial boundary value problem of linear momentum balance in conjunction with the product algorithm for the the constitutive equations is proposed. Numerical examples illustrate the effectiveness of the procedure.

1. Introduction

Constitutive equations appropriate for the finite deformation analysis of elastoplastic and elasto-viscoplastic materials are most frequently expressed in a spatial rate form. A thermodynamic framework for the development of such equations can be provided by characterizing irreversible processes through the use of internal variables [1,2,3,4]. In this case, spatial rate constitutive equations, expressed in terms of objective rates, will be required for the stress tensor and a set of internal variables. In any numerical scheme employed for the analysis of elastoplastic or elasto-viscoplastic problems it will be necessary to integrate these rate constitutive equations for the stress and internal variables. It is the object of this paper to derive adequate spatial rate constitutive equations for a limited class of elastoplastic and elasto-viscoplastic materials undergoing finite deformation and to propose a numerical algorithm for their integration.

The correct choice of objective rate appearing in spatial rate constitutive equations has been the subject of considerable conjecture [5,6,7,8] since the principle of objectivity alone does not uniquely determine this choice. It is noted, however, that the principles of mechanics must be invariant with respect to the choice of reference configuration [9]. When this principle is invoked together with the assumed existence of a free energy density, it is shown that the indeterminacy in the choice of objective rates for the spatial stress tensor and the spatial internal variables is removed.

A number of theories of plasticity have been based on different kinematic assumptions regarding the elastic-plastic split of the deformation [10,11,12]. A requirement for the success of the numerical integration algorithm proposed in this paper is that the spatial rate of deformation tensor admit an additive decomposition into an "elastic" and a "plastic" part. A thermodynamic argument for such a decomposition is provided within the framework of the internal variable theory.

The discussion of constitutive equations is concluded by the presentation of specific examples which are general enough to accomodate perfect and hardening viscoplasticity as well as perfect and hardening plasticity. In this paper, inviscid or rate-independent plasticity is treated as the limiting case of viscoplasticity as the viscosity of the material tends to zero or, alternatively, as an infinite length of time is allowed for the stress and internal variables to relax to their asymptotic values.

Following the development of the rate constitutive equations, a numerical algorithm is presented for their integration. As a consequence of the additive decomposition of the spatial rate of deformation tensor, the complete set of spatial rate constitutive equations also exhibits an additive decomposition into elastic and plastic parts. This "operator split" into component parts suggests the application of the product formula techniques for the construction of an efficient algorithm. Operator split methods have recently been successfully applied to the finite element analysis of problems in a number of areas. For example, the heat conduction problem [13], the structural dynamics problem [14] and in plasticity [15,16]. However, as will be made clear below, the application of the operator split method for plasticity reported in [15,16] is quite different to the approach being pursued in the present paper. After providing a brief general overview of product formula techniques, their application to the integration of rate constitutive equations is considered in detail. It is shown that the product algorithm consists of first integrating the elastic rate constitutive equations, ignoring the plasticity of the material. The stresses resulting from this operation are then allowed to relax towards the elastic domain, which itself is evolving according to the internal variable rate equations.

From a numerical point of view, an algorithm for the integration of rate constitutive equations should satisfy three requirements:

(i) Consistency with the constitutive equations.

(ii) Numerical stability.

(iii) Incremental objectivity.

Conditions (i) and (ii) are required for the convergence of the integration scheme [17]. Condition (iii) results from the physical requirement that the algorithm be invariant with respect to superimposed rigid body motion [18,19]. It is shown that the proposed product algorithm provides a basis for demonstrating the consistency and numerical stability of the resulting algorithm. The requirements of incremental objectivity are also considered in detail.

Although the development of global algorithms for the solution of the boundary value problem of linear momentum balance is outside the scope of the present paper, such algorithms provide the motivation for developing numerical schemes for the integration of the rate constitutive equations. Indeed, the two are strongly interdependent and cannot be entirely separated in any reasonably complete discussion of either algorithm. Accordingly, a brief description of global algorithms is presented. It is noted that "implicit" global algorithms which employ an elastoplastic (or elasto-viscoplastic) tangent modulus tensor suffer from certain computational disadvantages. These disadvantages lead to the development of alternative algorithms based on the operator split of the momentum balance equation [16]. Unfortunately, the error introduced into the product algorithm through the operator split tends to dominate at "practical" time step sizes. Refining the time step size for the global algorithm is very costly. In response, an implicit global algorithm is proposed in conjunction with the product formula algorithm for the constitutive equations which eliminates the disadvantages of the global implicit method resulting in an efficient and very accurate solution scheme.

In order to further improve the accuracy of the proposed algorithm, a method for refining the time step size in the product algorithm for the constitutive equations is presented. The time step size for the global algorithm is unaffected. This has the desirable effect of improving the accuracy (by reducing the error introduced by the operator split) of the overall scheme without incurring considerable cost, since the constitutive equations are integrated locally.

An interpretation of these algorithms for finite element analysis is considered throughout the development.

Finally, numerical examples are presented to demonstrate the effectiveness of the proposed algorithms.

2. Field Equations for Finite Deformation Elastoplasticity.

2.1. Preliminaries

A motion of a deformable body in the ambient space R^N, relative to a reference configuration B, is given by a time dependent mapping $\boldsymbol{\phi}_t(\mathbf{X}) : B \rightarrow R^N$, $t > 0$. Here, $\mathbf{X}$ denotes a set of material coordinates defined on the reference configuration.

The material velocity of the motion $\boldsymbol{\phi}_t$ is defined as a vector field $\mathbf{V}$ over the reference configuration, such that $\mathbf{V} = \frac{d}{dt}\boldsymbol{\phi}_t$ The spatial velocity field $\mathbf{v}$ is defined by $\mathbf{v} = \mathbf{V} \circ \boldsymbol{\phi}_t^{-1}$. Note that the spatial velocity field $\mathbf{v}(\mathbf{x}, t)$ is dependent on a set of spatial coordinates denoted $\mathbf{x}$.

The deformation gradient is defined by $\mathbf{F} = \dfrac{\partial \boldsymbol{\phi}}{\partial \mathbf{X}}$ with components, $F^a{}_A = \dfrac{\partial \phi^a}{\partial X^A}$. The polar decomposition of the deformation gradient is given by $\mathbf{F} = \mathbf{R} \cdot \mathbf{U} = \mathbf{V} \cdot \mathbf{R}$, where $\mathbf{R}$ is an orthogonal rotation tensor and $\mathbf{U}$ and $\mathbf{V}$ are respectively positive definite and symmetric right and left stretch tensors. From $\mathbf{F}$ one can obtain the Jacobian of the motion $J = \det \mathbf{F}$ and the right Cauchy-Green deformation tensor $\mathbf{C}$ which is related to the deformation gradient by $\mathbf{C} = \mathbf{F}^T \cdot \mathbf{F}$.

The spatial velocity gradient tensor $\mathbf{l}$ is given by $\mathbf{l} = \nabla \mathbf{v}$, where ∇ denotes the gradient with respect to the spatial coordinates $\mathbf{x}$. The symmetric part of $\mathbf{l}$, $\mathbf{d} \equiv \nabla^S \mathbf{v}$ is the spatial rate of deformation tensor, and the skewsymmetric part $\boldsymbol{\omega} \equiv \nabla^A \mathbf{v}$ is the spin rate or vorticity tensor.

If $\boldsymbol{\gamma}$ is a tensor field defined on the deformed configuration $\boldsymbol{\phi}_t(B)$, the pull back of $\boldsymbol{\gamma}$ through the motion $\boldsymbol{\phi}_t$ defines a tensor field $\boldsymbol{\Gamma}$ on B denoted by $\boldsymbol{\Gamma} = \boldsymbol{\phi}_t^*(\boldsymbol{\gamma})$ [9]. For example, in the case of a second order contravariant tensor the pull back operation takes the form

$$\Gamma^{AB} = (F^{-1})^A{}_a (F^{-1})^B{}_b (\gamma^{ab} \circ \boldsymbol{\phi}_t).$$

This definition may be readily generalized to spatial tensor fields of any order.

Likewise, if $\boldsymbol{\Gamma}$ is a material tensor field defined on B, the push forward of $\boldsymbol{\Gamma}$ through the motion $\boldsymbol{\phi}_t$ defines a spatial tensor field $\boldsymbol{\gamma}$ on $\boldsymbol{\phi}_t(B)$ denoted by $\boldsymbol{\gamma} = \boldsymbol{\phi}_{t*}(\boldsymbol{\Gamma})$. In this case, for the example used above, the push forward operation takes the form

$$\gamma^{ab} = F^a{}_A F^b{}_B (\Gamma^{AB} \circ \boldsymbol{\phi}_t^{-1}).$$

A related concept associated with the push forward of material rates of material tensors is that of the Lie derivative of a spatial tensor with respect to the spatial velocity field. The Lie derivative entails pulling back the spatial tensor to the reference configuration, taking the material time derivative of the resulting material tensor and pushing forward the result into the current configuration. Formally, for a spatial tensor $\boldsymbol{\gamma}$,

$$L_v(\boldsymbol{\gamma}) \equiv \boldsymbol{\phi}_{t*}\left[\frac{d}{dt}\boldsymbol{\phi}_t^{*}(\boldsymbol{\gamma})\right] \tag{1}$$

This notation allows for a compact expression of many relations in continuum mechanics. For example, the Cauchy stress tensor $\boldsymbol{\sigma}$ defined on the current configuration and the second Piola-Kirchhoff stress tensor $\mathbf{S}$ associated with the reference configuration are related by

$$\mathbf{S} = J\boldsymbol{\phi}_t^{*}(\boldsymbol{\sigma}) \quad or \quad \boldsymbol{\sigma} = \boldsymbol{\phi}_{t*}(J^{-1}\mathbf{S})$$

These relations, involving J, are called Piola transformations.

The forward Piola transformation of the material time derivative of $\mathbf{S}$, denoted $\overset{\circ}{\boldsymbol{\sigma}}$, is

$$\overset{\circ}{\boldsymbol{\sigma}} = \boldsymbol{\phi}_{t*}(J^{-1}\dot{\mathbf{S}}), \tag{2}$$

the so-called Truesdell rate of Cauchy stress. For contravariant components (2) has the form

$$\overset{\circ}{\boldsymbol{\sigma}} = \dot{\boldsymbol{\sigma}} - \mathbf{l}\cdot\boldsymbol{\sigma} - \boldsymbol{\sigma}\cdot\mathbf{l}^T + \boldsymbol{\sigma}\, tr(\mathbf{d}) \tag{3}$$

where $\dot{\boldsymbol{\sigma}}$ denotes the material time derivative of $\boldsymbol{\sigma}$ given by $\dot{\boldsymbol{\sigma}} = \dfrac{\partial\boldsymbol{\sigma}}{\partial t} + \nabla\boldsymbol{\sigma}\cdot\mathbf{v}$. Alternatively, in terms of the Lie derivative, (2) can be written

$$\overset{\circ}{\boldsymbol{\sigma}} = J^{-1}\boldsymbol{\phi}_{t*}\left[\frac{d}{dt}\boldsymbol{\phi}_t^{*}(J\boldsymbol{\sigma})\right] = J^{-1}L_v(\boldsymbol{\tau}) \tag{4}$$

where $\boldsymbol{\tau} \equiv (J\circ\boldsymbol{\phi}_t^{-1})\,\boldsymbol{\sigma}$ is the Kirchhoff stress tensor.

The principle of objectivity requires that intrinsic physical properties of a body be independent of the body's location or orientation in space. This principle is embodied in constitutive theory by requiring that constitutive equations contain only objective tensor fields. Consequently, since the Truesdell rate is objective [9,20] it may be considered as a candidate for use in spatial rate constitutive equations.

Many other objective rates have been proposed within the context of constitutive theory. One that frequently arises is the Jaumann, or co-rotational rate of Kirchhoff stress,

$$\overset{\nabla}{\boldsymbol{\tau}} = \dot{\boldsymbol{\tau}} - \boldsymbol{\omega}\cdot\boldsymbol{\tau} + \boldsymbol{\tau}\cdot\boldsymbol{\omega} \tag{5}$$

The co-rotational rate can be related to the Lie derivative. To explicate this relationship, pull back and push forward operations associated with the rotational part of the deformation gradient, or co-rotational pull back and push forward operations, are introduced as follows. Given any spatial tensor $\boldsymbol{\gamma}$, the co-rotational pull back of $\boldsymbol{\gamma}$, $\boldsymbol{\phi}_t^{R*}(\boldsymbol{\gamma})$, is defined by formally replacing the deformation gradient appearing in the pull back operation by its rotational component tensor $\mathbf{R}$. The co-rotational push forward operation is similarly defined. With this notation, the Jaumann or co-rotational rate of Kirchhoff stress is given by

$$\overset{\nabla}{\boldsymbol{\tau}} = \boldsymbol{\phi}_{t*}^{R}\left[\frac{d}{dt}\boldsymbol{\phi}_t^{R*}(\boldsymbol{\tau})\right] \tag{6}$$

Comparing this expression with (1) it is noted that the Jaumann rate coincides with the Lie derivative under the assumption that the rate of deformation tensor vanishes, that is

$$\overset{\nabla}{\boldsymbol{\tau}} = L_{\mathbf{v}}(\boldsymbol{\tau})\big|_{\mathbf{d}=0} \tag{7}$$

Noting that $\dot{\mathbf{F}} = \boldsymbol{\omega}\cdot\mathbf{F}$ when $\mathbf{d} = 0$, where $\boldsymbol{\omega}$ is the spin rate tensor, it follows that

$$L_{\mathbf{v}}(\boldsymbol{\tau})\big|_{\mathbf{d}=0} = \dot{\boldsymbol{\tau}} - \boldsymbol{\omega}\cdot\boldsymbol{\tau} - \boldsymbol{\tau}\cdot\boldsymbol{\omega}^T = \overset{\nabla}{\boldsymbol{\tau}}$$

for contravariant components of $\boldsymbol{\tau}$.

Finally, the local form of linear momentum balance together with traction and kinematic boundary conditions can be expressed as

$$\begin{aligned} \rho\,\dot{\mathbf{v}} &= \nabla\cdot\boldsymbol{\sigma} + \rho\,\mathbf{b} \qquad \mathbf{x}\in\boldsymbol{\phi}_t(B) \\ \boldsymbol{\sigma}\cdot\mathbf{n} &= \bar{\mathbf{t}} \qquad \mathbf{x}\in\partial_\sigma\boldsymbol{\phi}_t(B) \\ \boldsymbol{\phi} &= \bar{\boldsymbol{\phi}} \qquad \mathbf{x}\in\partial_u\boldsymbol{\phi}_t(B) \end{aligned} \tag{8}$$

where ρ is the mass density in $\boldsymbol{\phi}_t(B)$, $\mathbf{b}$ is a spatial body force field, and $\bar{\mathbf{t}}$ and $\bar{\boldsymbol{\phi}}$ are the prescribed tractions and motion over the traction and kinematic boundaries $\partial_\sigma\boldsymbol{\phi}_t(B)$ and $\partial_u\boldsymbol{\phi}_t(B)$, respectively.

Suitable constitutive equations need to be introduced in order to complete the specification of an initial boundary value problem. The form of these equations for a limited class of elastoplastic and elasto-viscoplastic materials is the subject of the next section.

2.2. Rate Constitutive Equations for Finite Deformation Elastoplasticity and Elasto-Viscoplasticity

Constitutive equations appropriate for the finite deformation analysis of elastoplastic and elasto-viscoplastic materials are most frequently expressed in a spatial rate form. A thermodynamic framework for the development of such equations can be provided by characterizing irreversible processes through the use of internal variables [1,2,3,4]. In this case, spatial rate constitutive equations will be required for the stress tensor and a set of internal variables.

Rate constitutive equations can be alternatively formulated in a material or a spatial setting. The former case involves rates of material tensors which are always objective. In a spatial formulation, however, material rates of objective tensors are not objective and objective stress rates, such as the Truesdell or Jaumann rates, must be introduced. The approach taken here is based on a thermodynamic formulation in a material setting, the spatial representation of which is then consistently derived. As noted in Section 1, the correct choice of objective rate appearing in spatial rate constitutive equations has been the subject of considerable conjecture [5,6,7,8] since the principle of objectivity alone does not uniquely determine this choice. It is demonstrated below, however, that when the invariance of constitutive equations to the choice of reference configuration is invoked together with the assumed existence of a free energy density, the indeterminacy in the choice of objective rates for the spatial stress tensor and the spatial internal variables is removed.

A number of theories of plasticity have been based on different kinematic assumptions regarding the elastic-plastic split of the deformation [10,11,12]. A requirement for the success of the numerical integration algorithm proposed in this paper is that the spatial rate of deformation tensor admit an additive decomposition into an "elastic" and a "plastic" part. A thermodynamic argument for such a decomposition is provided within the framework of the internal variable theory.

The existence of a complementary free energy potential per unit mass of B, denoted $\chi(\mathbf{S},\mathbf{Q}_1,\mathbf{Q}_2,\ldots,\mathbf{Q}_{niv})$ is assumed. Here, $\mathbf{S}$ is the second Piola-Kirchhoff stress tensor and $\{\mathbf{Q}_\alpha\}$, $\alpha = 1,\ldots,niv$, is a set of internal variables, the members of which may be scalars or tensors of any order, defined on the reference configuration B. The justification for such an assumption is argued in [21].

Assuming only mild restrictions on the structure of the internal variable rate constitutive equations [21], it can be shown from the Clausius-Duhem inequality [21,23] that the complementary free energy density is a potential for the right Cauchy-Green deformation tensor $\mathbf{C}$, i.e.,

$$\mathbf{C} = 2\rho_o \frac{\partial \chi}{\partial \mathbf{S}} \tag{9}$$

where ρ_o denotes the reference mass density. A rate form of (9) is obtained by taking the material time derivative, resulting in

$$\dot{\mathbf{C}} = \mathbf{M}:\dot{\mathbf{S}} + \sum_{\alpha=1}^{niv} \mathbf{N}_\alpha \cdot \dot{\mathbf{Q}}_\alpha \tag{10}$$

where $\mathbf{M}$ is the elastic compliance tensor defined by

$$\mathbf{M} = 2\rho_o \frac{\partial^2 \chi}{\partial \mathbf{S}^2} \tag{11}$$

and $\mathbf{N}_\alpha$ is an inelastic compliance tensor defined by

$$\mathbf{N}_\alpha = 2\rho_o \frac{\partial^2 \chi}{\partial \mathbf{Q}_\alpha \partial \mathbf{S}}. \tag{12}$$

In (10), the contraction $\mathbf{N}_\alpha \cdot \dot{\mathbf{Q}}_\alpha$ is to be interpreted according to the order of $\mathbf{Q}_\alpha$. Since material time derivatives of material tensors are objective, constitutive equation (10) is also objective.

A spatial form of constitutive eq. (10) can be obtained as follows. Noting that

$$\dot{\mathbf{C}} = 2\boldsymbol{\phi}_t^*(\mathbf{d}), \tag{13}$$

recalling (2) and introducing spatial internal variables $\mathbf{q}_\alpha = \boldsymbol{\phi}_{t*}(J^{-1}\mathbf{Q}_\alpha)$, the Truesdell rate of which is given by $\overset{\circ}{\mathbf{q}}_\alpha = \boldsymbol{\phi}_{t*}(J^{-1}\dot{\mathbf{Q}}_\alpha)$, equation (10) has the alternative form

$$2\boldsymbol{\phi}_t^*(\mathbf{d}) = J\,\mathbf{M}:\boldsymbol{\phi}_t^*(\overset{\circ}{\boldsymbol{\sigma}}) + \sum_{\alpha=1}^{niv} J\,\mathbf{N}_\alpha \cdot \boldsymbol{\phi}_t^*(\overset{\circ}{\mathbf{q}}_\alpha). \tag{14}$$

The push forward of (14) reads

$$\mathbf{d} = \mathbf{m}:\overset{\circ}{\boldsymbol{\sigma}} + \sum_{\alpha=1}^{niv} \mathbf{n}_\alpha \cdot \overset{\circ}{\mathbf{q}}_\alpha \tag{15}$$

where $\mathbf{m} = \frac{1}{2} J \boldsymbol{\phi}_{t*}(\mathbf{M})$ is the spatial elastic compliance tensor and $\mathbf{n}_\alpha = \frac{1}{2} J \boldsymbol{\phi}_{t*}(\mathbf{N}_\alpha)$ is a spatial inelastic compliance tensor. The material and spatial forms, (10) and (15) respectively, must be equivalent and simply represent alternative expressions of the same constitutive hypothesis. This equivalence is required by the principle that the laws of continuum mechanics must be invariant with respect to the choice of reference configuration. It is interesting to note that this invariance principle uniquely determines the form of the spatial rate constitutive equations. In particular, the Truesdell rate of Cauchy stress appears as a natural choice of objective spatial stress rate consistent with the material formulation.

Furthermore, equation (15) has the interpretation that the rate of deformation tensor $\mathbf{d}$ has an additive decomposition into an "elastic" part $\mathbf{d}^e = \mathbf{m}:\overset{\circ}{\boldsymbol{\sigma}}$ and an "inelastic" or "plastic" part $\mathbf{d}^p = \sum_{\alpha=1}^{niv} \mathbf{n}_\alpha \cdot \overset{\circ}{\mathbf{q}}_\alpha$, that is

$$\mathbf{d} = \mathbf{d}^e + \mathbf{d}^p. \tag{16}$$

This decomposition has been obtained independently of any kinematic considerations. Other theories of plasticity based on specific kinematic assumptions [10,11,12] can be brought into correspondence with (16) by appropriate definitions of the kinematic variables. Combining (15) and (16), it follows that

$$\begin{aligned} \overset{\circ}{\boldsymbol{\sigma}} &= \mathbf{a} : (\mathbf{d} - \mathbf{d}^p) \\ \mathbf{d}^p &= \sum_{\alpha=1}^{niv} \mathbf{n}_\alpha \cdot \overset{\circ}{\mathbf{q}}_\alpha \end{aligned} \tag{17}$$

where $\mathbf{a} = \mathbf{m}^{-1}$ is the spatial elastic modulus tensor.

It is noted that (17) is expressible in terms of other stress rates if the difference between these rates and the Truesdell rate of Cauchy stress is absorbed in the definition of the elastic modulus tensor. In this case, the modified elastic modulus tensor will, in general, be a function of the deformation and the spatial stress tensor [19,20].

In order to have a complete set of constitutive equations one has to supplement (17) with constitutive relations for $\overset{\circ}{\mathbf{q}}_\alpha$ as well as supplying the functional form of the spatial compliances $\mathbf{m}$ and $\mathbf{n}_\alpha$. The "rate-dependent" or "rate-independent" characterization of plasticity will reside in the structure of the constitutive equations for $\overset{\circ}{\mathbf{q}}_\alpha$ [21]. If these rate constitutive equations are homogeneous (of degree one) in some measure of time then rate-independent (inviscid plastic) behavior is obtained, otherwise rate-dependent (viscoplastic) behavior results. The constitutive equations for $\overset{\circ}{\mathbf{q}}_\alpha$ can not be specified arbitrarily but must satisfy

$$\sum_{\alpha=1}^{niv} J \phi_{t*}\left(\frac{\partial \chi}{\partial \mathbf{Q}_\alpha}\right) : \overset{\circ}{\mathbf{q}}_\alpha \geqslant 0$$

which is a representation of the Clausius-Planck dissipation inequality [21,23].

For the present purpose it will suffice to assume that $\mathbf{d}^p$ can be expressed as a function of the spatial stress and the spatial internal variables

$$\mathbf{d}^p = \mathrm{T}(\boldsymbol{\sigma}, \mathbf{q}_1, \ldots, \mathbf{q}_{niv}), \tag{18}$$

where the internal variables $\mathbf{q}_\alpha$ may for example represent some invariant of the yield stress for an isotropic hardening model or the translation of the elastic domain for a kinematic hardening model.

We introduce here two particularly simple examples of the constitutive mapping **T** appearing in (18).

2.2.1. Perfect Viscoplasticity

For a perfectly viscoplastic material we first introduce a closed convex elastic domain C in stress space $S \equiv R^6$ which contains the origin and has a smooth boundary ∂C. Then, for every point $\boldsymbol{\sigma} \in S$, we assume constitutive equation (18) has the form

$$\mathbf{T}(\boldsymbol{\sigma}) = \begin{cases} \lambda\, \mathbf{n}_\sigma & \text{if} \boldsymbol{\sigma} \in S - Int(C) \\ 0 & \text{if} \boldsymbol{\sigma} \in Int(C) \end{cases} \tag{19}$$

where $\mathbf{n}_\sigma$ is the outward normal to ∂C at the (unique) point on ∂C which is closest to $\boldsymbol{\sigma}$, $\lambda \geqslant 0$ and $Int(C) = C - \partial C$. Note that no internal variables are required for this model. Equation (19) may be viewed as a generalization of the usual normality assumption of infinitesimal plasticity.

A specific example of such a constitutive equation can be constructed as follows. Given any point $\boldsymbol{\sigma} \in S$, then from the assumed convexity of C, there is always a unique point $\mathbf{P}_C \boldsymbol{\sigma}$ in C which is closest to $\boldsymbol{\sigma}$. The mapping $\mathbf{P}_C$ is called the closest point mapping (relative to C). Clearly, if $\boldsymbol{\sigma} \in C$ then $\mathbf{P}_C \boldsymbol{\sigma} = \boldsymbol{\sigma}$. If, on the other hand, $\boldsymbol{\sigma} \in S - C$ then $\boldsymbol{\sigma} - \mathbf{P}_C \boldsymbol{\sigma} = \mu\, \mathbf{n}_\sigma$ with $\mu > 0$. This suggests taking the viscoplastic constitutive mapping (19) in the form

$$\mathbf{T}(\boldsymbol{\sigma}) = \frac{\boldsymbol{\sigma} - \mathbf{P}_C \boldsymbol{\sigma}}{\eta} \tag{20}$$

The parameter η is the viscosity of the material. If $\boldsymbol{\sigma}$ belongs to C then $\mathbf{P}_C \boldsymbol{\sigma} = \boldsymbol{\sigma}$ and $\mathbf{d}^p = \mathbf{T}(\boldsymbol{\sigma}) = 0$. If, on the other hand, $\boldsymbol{\sigma}$ does not belong to C then $\mathbf{d}^p$ is directed along the vector that joins $\boldsymbol{\sigma}$ and its closest point in C and it points outside the elastic region. The magnitude of $\mathbf{d}^p$ is proportional to the distance from $\boldsymbol{\sigma}$ to C, the proportionality constant being $\dfrac{1}{\eta}$, Fig. 1. It clear that (20) is also well behaved (single valued) when ∂C is not smooth but exhibits corners, Fig. 1. Examples employing the von Mises yield criterion in the definition of the elastic domain C are given in Section 3.

In this paper, inviscid or rate-independent plasticity is treated as the limiting case of viscoplasticity as the viscosity η of the material tends to zero. Alternatively, one may think of this limiting process as the result of allowing an infinite period of time to elapse for the relaxation of the stresses towards the elastic region. Examples of this process are considered in Section 3.

2.2.2. Hardening Viscoplasticity

In the case of hardening viscoplasticity, a set of spatial internal variables $\mathbf{q} \equiv \{\mathbf{q}_\alpha\}$, $\alpha = 1, \ldots, niv$ is introduced such that the elastic domain $C(\mathbf{q})$ now depends on the current values of the internal variables. The plastic constitutive mapping (20) can be generalized for this case by taking

$$\mathbf{T}(\boldsymbol{\sigma},\mathbf{q}) = \frac{\boldsymbol{\sigma} - \mathbf{P}_{C(\mathbf{q})}\boldsymbol{\sigma}}{\eta} \tag{21}$$

where $\mathbf{P}_{C(\mathbf{q})}$ denotes the closest point mapping relative to $C(\mathbf{q})$.

It is assumed in this hardening case that the evolution of the internal variables is governed by evolutionary equations of the form

$$\overset{\circ}{\mathbf{q}}_\alpha = \mathbf{f}_\alpha(\boldsymbol{\sigma},\mathbf{q}_1, \ldots ,\mathbf{q}_{niv}), \quad \alpha = 1,\ldots, niv \tag{22}$$

Note that the use of the Truesdell rate in the left hand side of (22) makes these equations objective and consistent with a set of material kinetic equations given by $\dot{\mathbf{Q}}_\alpha = \mathbf{H}_\alpha(\mathbf{S},\mathbf{Q}_1, \ldots ,\mathbf{Q}_{niv})$ where $\mathbf{f}_\alpha = \boldsymbol{\phi}_{t*}(J^{-1}\mathbf{H}_\alpha)$.

As for the case of perfect (inviscid) plasticity, hardening plasticity will be treated as the limiting case of hardening viscoplasticity as the viscosity η of the material tends to zero or, alternatively, as an infinite period of time is allowed for the stress and internal variables to relax to their asymptotic values. Examples of this process are considered in the following section.

3. Numerical Integration of Rate Constitutive Equations for Elastoplasticity and Elasto-Viscoplasticity

3.1. Introduction

As noted in the Introduction, any numerical scheme for the solution of the boundary value problem of linear momentum balance for elastoplastic or elasto-viscoplastic materials will require an algorithm for the integration of the rate constitutive equations. This section addresses the numerical integration of rate constitutive equations for the stress and internal variables introduced in Section 2 and summarized from (17), (18) and (22) as

$$\begin{aligned} \overset{\circ}{\boldsymbol{\sigma}} &= \mathbf{a} : (\mathbf{d} - \mathbf{T}(\boldsymbol{\sigma},\mathbf{q}_1, \ldots ,\mathbf{q}_{niv})) \\ \overset{\circ}{\mathbf{q}}_\alpha &= \mathbf{f}_\alpha(\boldsymbol{\sigma},\mathbf{q}_1, \ldots ,\mathbf{q}_{niv}), \ \alpha = 1,\ldots, niv \end{aligned} \tag{23}$$

As a consequence of the additive decomposition of the spatial rate of deformation tensor (16), constitutive equations (23) also exhibit an additive decomposition into an elastic part

$$\begin{aligned} \overset{\circ}{\boldsymbol{\sigma}} &= \mathbf{a} : \mathbf{d} \\ \partial \mathbf{q}_\alpha / \partial t &= 0, \quad \alpha = 1,\ldots, niv \end{aligned} \tag{24}$$

and a plastic part

$$\begin{aligned} \partial \boldsymbol{\sigma} / \partial t &= -\mathbf{a} : \mathbf{T}(\boldsymbol{\sigma},\mathbf{q}_1, \ldots ,\mathbf{q}_{niv}) \\ \overset{\circ}{\mathbf{q}}_\alpha &= \mathbf{f}_\alpha(\boldsymbol{\sigma},\mathbf{q}_1, \ldots ,\mathbf{q}_{niv}), \quad \alpha = 1,\ldots, niv \end{aligned} \tag{25}$$

From a numerical point of view, an algorithm for the integration of (23) should satisfy three requirements:

(i) Consistency with the constitutive equations.

(ii) Numerical stability.

(iii) Incremental objectivity.

Conditions (i) and (ii) are required for the convergence of the numerical integration scheme [17]. Condition (iii) results from the physical requirement that the algorithm must be invariant with respect to superimposed rigid body motions. This idea is considered in detail in subsequent sections. Few algorithms reported in the literature seem to satisfy all these requirements.

Equations (24) and (25) suggest the possibility of using product formula techniques for constructing efficient solution algorithms for (23) which will also provide a basis for demonstrating the consistency and numerical stability of the resulting algorithms. Before presenting the details of such an algorithm a brief discussion of general product algorithms will be useful.

3.2. Operator Splits and Product Algorithms

The operator split method has recently been applied to the finite element analysis of the heat conduction problem [13], to the structural dynamics problem [14] and also, as discussed above, to the finite deformation elastoplastic dynamic problem [16]. A collection of results regarding operator split methods and product formula algorithms for general nonlinear equations of evolution is presented in [13,14]. These results illustrate the point that product formulas can be advantageously applied to any set of equations of evolution where the evolutionary operator has an additive decomposition (operator split) into component operators. The basic idea underlying product formulas is that 'of treating each one of the component operators independently. In a typical integration process, one applies an algorithm to the solution vector that is consistent with the first component operator, the result of which is then operated upon with an algorithm which is consistent with the second component operator, and so on.

Consider the following general evolution equation

$$\mathbf{A}\,\dot{\mathbf{x}} + \mathbf{B}(\mathbf{x}) = \mathbf{f} \;; \quad \mathbf{x}(0) = \mathbf{x}_o \tag{26}$$

where $\mathbf{x}$ is an s-dimensional vector, $\mathbf{A}$ is a positive definite symmetric matrix and $\mathbf{B}$ is a nonlinear function from R^s into R^s. We endow R^s with the "energy" inner product $<\mathbf{x},\mathbf{y}> = \mathbf{x}^T\mathbf{A}\mathbf{y}$ for every $\mathbf{x},\mathbf{y} \in R^s$, with its associated norm $||\mathbf{x}||^2 = <\mathbf{x},\mathbf{x}>$. In this context, an unconditionally stable algorithm for equation (26) is a one-parameter family of (nonlinear) functions $\mathbf{F}(h) : R^s \rightarrow R^s$, $h > 0$, satisfying

1) Consistency:

$$\lim_{h \to 0^+} \mathbf{A} \frac{\mathbf{F}(h)\mathbf{x} - \mathbf{x}}{h} = \mathbf{B}(\mathbf{x}) + \mathbf{f} \quad \textit{for every} \;\; \mathbf{x} \in R^s \tag{27}$$

2) Unconditional stability:

$$||\mathbf{F}(h)\,\mathbf{x} - \mathbf{F}(h)\,\mathbf{y}|| \leqslant ||\mathbf{x} - \mathbf{y}|| \quad \textit{for every} \;\; \mathbf{x},\mathbf{y} \in R^s, \;\; h>0. \tag{28}$$

If $\mathbf{F}(h)$ is a consistent and stable algorithm for (26) in the sense of (27) and (28) then convergence is guaranteed under mild conditions on $\mathbf{B}$ [17].

Suppose the evolutionary operator $\mathbf{B}$ and the forcing term $\mathbf{f}$ admit an additive decomposition

$$\mathbf{B} = \sum_{i=1}^{N} \mathbf{B}_i \quad ; \quad \mathbf{f} = \sum_{i=1}^{N} \mathbf{f}_i. \tag{29}$$

and let $\mathbf{F}_i(h)$, $i = 1,2, \cdots, N$ denote stable algorithms consistent with

$$\mathbf{A}\,\dot{\mathbf{x}} + \mathbf{B}_i(\mathbf{x}) = \mathbf{f}_i.$$

Then the corresponding global product algorithm takes the form

$$\mathbf{F}(h) = \mathbf{F}_N(h)\,\mathbf{F}_{N-1}(h) \cdots \mathbf{F}_1(h) \equiv \prod_{i=1}^{N} \mathbf{F}_i(h) \tag{30}$$

In other words, the algorithm $\mathbf{F}(h)$ amounts to applying the individual algorithms $\mathbf{F}_i(h)$ consecutively to the solution vector, taking the result from each one of these applications as the initial conditions for the next algorithm. The global algorithm is complete for a given time step when all the individual algorithms have been applied.

It can be shown that if all the individual algorithms $\mathbf{F}_i(h)$ are consistent with $\mathbf{A}$, $\mathbf{B}_i$ and $\mathbf{f}_i$ in the sense of (27), then the global product algorithm $\mathbf{F}(h)$ given by (30) is consistent with $\mathbf{A}$, $\mathbf{B}$ and $\mathbf{f}$ [14]. It can also be shown that if all the individual algorithms $\mathbf{F}_i(h)$ are unconditionally stable in the sense of (28), then the global product algorithm $\mathbf{F}(h)$ is also unconditionally stable [14]. In other words the norm stability of the individual algorithms, in the sense of (28), is preserved by the product formula (30). A general discussion of these and other related issues can be found in [13,14].

3.3. A Product Algorithm for Rate Constitutive Equations

A product algorithm for the integration of the rate constitutive equations (23) relative to the additive decomposition given by (24) and (25) can be constructed as follows. Consider two unconditionally stable algorithms $\mathbf{F}^{el}(h)$ and $\mathbf{F}^{pl}(h)$ which are consistent, in the sense of (27), with (24) and (25) respectively. Then an unconditionally stable algorithm $\mathbf{F}(h)$ which is consistent with the complete set of constitutive equations (23) is given, in analogy with (30), by

$$\mathbf{F}(h) = \mathbf{F}^{pl}(h)\,\mathbf{F}^{el}(h) \tag{31}$$

such that

$$\mathbf{F}(h)\begin{Bmatrix}\boldsymbol{\sigma}\\ \mathbf{q}_\alpha\end{Bmatrix} = \mathbf{F}^{pl}(h)\left\{\mathbf{F}^{el}(h)\begin{Bmatrix}\boldsymbol{\sigma}\\ \mathbf{q}_\alpha\end{Bmatrix}\right\} = \begin{Bmatrix}\boldsymbol{\sigma}(h)\\ \mathbf{q}_\alpha(h)\end{Bmatrix}, \quad \alpha = 1,\ldots, niv.$$

The product formula (31) states that a solution algorithm is obtained by first integrating the elastic constitutive equations and then applying to the solution vector so obtained a plastic algorithm operating on the stress and internal variables reflecting the effect of the plastic part of the constitutive equations. The remainder of this section is concerned with the development of the $\mathbf{F}^{el}(h)$ and $\mathbf{F}^{pl}(h)$ algorithms.

3.3.1. Elastic Algorithm

The desired algorithm $\mathbf{F}^{el}(h)$ must be unconditionally stable and consistent with (24) in the sense of (27). It is observed that the evolution equations (24) affect only the stresses with the internal variables $\mathbf{q}_\alpha$ remaining constant, thus the algorithm can be expressed as

$$\mathbf{F}^{el}(h)\begin{Bmatrix}\boldsymbol{\sigma}\\ \mathbf{q}_\alpha\end{Bmatrix} = \begin{Bmatrix}\boldsymbol{\sigma}(h)\\ \mathbf{q}_\alpha\end{Bmatrix}, \quad \alpha = 1,\ldots niv. \tag{32}$$

Objective rates appearing in spatial constitutive equations have the effect of introducing some complications in the development of numerical integration algorithms and have motivated research on this problem [18,24,25]. However, few algorithms presented in the computational literature appear to be consistent with the constitutive equations which they are purporting to integrate. A family of algorithms, appropriate for the integration of (24), which does satisfy the requirements of consistency, numerical stability and incremental objectivity, has recently been proposed in [19]. The essential ideas are as follows. We start by noting that from a mathematical point of view, the usual linear space operations such as addition and scalar multiplication can only be rigorously applied to relate tensor fields associated with a common configuration [19]. It is thus natural to use the idea of pulling back spatial quantities to a common reference configuration in order to define difference operators to be used in numerical algorithms. This suggests defining algorithms for the integration of (24.a) based upon difference operators employing the second Piola-Kirchhoff stress tensor. A generalized mid-point rule algorithm can be introduced as follows:

$$\mathbf{S}_{n+1} - \mathbf{S}_n = h\,\dot{\mathbf{S}}_{n+\alpha} \quad 0 \leqslant \alpha \leqslant 1 \tag{33}$$

where subscripts refer to the time step, the time step size $h = t_{n+1} - t_n$ and $\dot{\mathbf{S}}_{n+\alpha}$ is to be evaluated on an intermediate configuration defined by the mapping $\boldsymbol{\phi}_{n+\alpha}(\mathbf{X}) : B \rightarrow R^N$ with

$$\boldsymbol{\phi}_{n+\alpha} = \alpha \boldsymbol{\phi}_{n+1} + (1-\alpha)\,\boldsymbol{\phi}_n \quad 0 \leqslant \alpha \leqslant 1 \tag{34}$$

Using the inverse of (2) and noting again that $\mathbf{S} = J\boldsymbol{\phi}_t^{*}(\boldsymbol{\sigma})$, (33) has the alternative representation

$$\boldsymbol{\phi}^{*}_{n+1}(J\boldsymbol{\sigma}) - \boldsymbol{\phi}^{*}_{n}(J\boldsymbol{\sigma}) = h\,\boldsymbol{\phi}^{*}_{n+\alpha}(J\overset{\circ}{\boldsymbol{\sigma}}) \tag{35}$$

To simplify (35) the reference configuration B is selected to coincide instantaneously with the configuration at time t_{n+1} such that $\boldsymbol{\phi}_{n+1} = \mathbf{I}$, in which case (35) reduces to

$$\boldsymbol{\sigma}_{n+1} - \boldsymbol{\phi}^{*}_{n}(J\boldsymbol{\sigma}) = h\,\boldsymbol{\phi}^{*}_{n+\alpha}(J\overset{\circ}{\boldsymbol{\sigma}}) \tag{36}$$

Defining the deformation gradients

$$\boldsymbol{\Lambda}_{n+\alpha} = \left(\frac{\partial \boldsymbol{\phi}_{n+\alpha}}{\partial \mathbf{x}_{n+1}}\right)^{-1} \quad 0 \leqslant \alpha \leqslant 1 \tag{37}$$

and Jacobians

$$J_{n+\alpha} = \det(\boldsymbol{\Lambda}_{n+\alpha}) \quad 0 \leqslant \alpha \leqslant 1 \tag{38}$$

then, for contravariant components of stress, (36) has the form

$$\boldsymbol{\sigma}_{n+1} - J_n^{-1}\boldsymbol{\Lambda}_n \cdot \boldsymbol{\sigma}_n \cdot \boldsymbol{\Lambda}_n^T = h\,J_{n+\alpha}^{-1}\,\boldsymbol{\Lambda}_{n+\alpha} \cdot \overset{\circ}{\boldsymbol{\sigma}}_{n+\alpha} \cdot \boldsymbol{\Lambda}_{n+\alpha}^T \tag{39}$$

This equation is completed by introducing the rate constitutive equation for $\overset{\circ}{\boldsymbol{\sigma}}_{n+\alpha}$. For example, for constitutive equation (24.a), eq. (39) is expressed by

$$\boldsymbol{\sigma}_{n+1} - J_n^{-1}\boldsymbol{\Lambda}_n \cdot \boldsymbol{\sigma}_n \cdot \boldsymbol{\Lambda}_n^T = h\,J_{n+\alpha}^{-1}\,\boldsymbol{\Lambda}_{n+\alpha} \cdot (\mathbf{a} : \mathbf{d})\big|_{n+\alpha} \cdot \boldsymbol{\Lambda}_{n+\alpha}^T \tag{40}$$

This form requires evaluation of the quantities $\boldsymbol{\Lambda}_{n+\alpha}$, $\mathbf{a}_{n+\alpha}$ and $\mathbf{d}_{n+\alpha}$. Assuming $\boldsymbol{\Lambda}_n$ to be a known quantity (representing the incremental motion for which the corresponding stresses are desired), it is shown in [19] that $\boldsymbol{\Lambda}_{n+\alpha}$ is given by

$$\boldsymbol{\Lambda}_{n+\alpha} = [(1-\alpha)\,\mathbf{I} + \alpha\,\boldsymbol{\Lambda}_n]^{-1} \cdot \boldsymbol{\Lambda}_n \tag{41}$$

and that $\mathbf{d}_{n+\alpha}$ is consistently approximated by

$$\mathbf{d}_{n+\alpha} = \frac{1}{h}\left[\left\{(1-\alpha)\mathbf{I} + \alpha\Lambda_n\right\}^{-1}\left\{\Lambda_n - \mathbf{I}\right\}\right]^S \tag{42}$$

As noted above, the algorithm (40) - (42) must to satisfy the three requirements of consistency with the spatial rate constitutive equations, numerical stability and incremental objectivity. It is demonstrated in [19] that the above algorithm is consistent with the rate constitutive equation and that it is unconditionally stable for $\alpha \geqslant 0.5$, moreover, it is second order accurate for $\alpha = 0.5$.

The condition of incremental objectivity is a physical requirement expressing the fact that the algorithm has to be invariant with respect to superimposed rigid body motions occurring over the time step and has the effect of restricting the admissible values of α. This idea was first expressed in an algorithmic context in [18] and further considered in [18,19]. Formally, let $\mathbf{R}$ be the group of all orthogonal second order tensors and $\mathbf{M}$ the group of all positive definite symmetric second order tensors. The algorithm defined by (40) - (42) is incrementally objective if and only if

$$(a) \quad \Lambda_n \in \mathbf{R} <=> \mathbf{d}_{n+\alpha} = 0$$

$$(b) \quad \Lambda_n \in \mathbf{M} <=> \boldsymbol{\omega}_{n+\alpha} = 0$$

where $\boldsymbol{\omega}_{n+\alpha}$ is the spin rate tensor determined by replacing the symmetric part on the right hand side of (42) by the skewsymmetric part. Condition (a) ensures that the integration algorithm reduces to $\boldsymbol{\sigma}_{n+1} = \Lambda_n \cdot \boldsymbol{\sigma}_n \cdot \Lambda_n^T$ in the event that $\Lambda_n \in \mathbf{R}$. It is demonstrated in [19] that the algorithm (40) - (42) is incrementally objective if and only if $\alpha = 0.5$.

Equation (40) may easily be generalized to accommodate choices of objective stress rate other than the Truesdell rate of Cauchy stress by embedding the difference between the stress rate definitions in the elastic modulus tensor $\mathbf{a}$. In this case (40) will, in general, become implicit in $\boldsymbol{\sigma}_{n+1}$ and may be solved by means of an iterative solution procedure [19]. The algorithm (40) - (42) fits naturally into a finite element implementation since it employs quantities that are readily available from standard shape function routines [20].

It is noted finally that the incrementally objective algorithm introduced in [18] can be related to the present algorithm (40) - (42), by replacing the pull back operations in (35) by their co-rotational counterparts and using the fact that the Lie derivative and the Jaumann rate coincide under the assumption that the rate of deformation tensor vanishes (see Section 2.1) [20]. This relation can be used to draw conclusions about the applicability of the algorithm presented in [18].

3.3.2. Plastic / Viscoplastic Algorithm

The desired algorithm $\mathbf{F}^{pl}(h)$, which can be expressed by

$$\mathbf{F}^{pl}(h)\begin{Bmatrix}\boldsymbol{\sigma}\\ \mathbf{q}_\alpha\end{Bmatrix} = \begin{Bmatrix}\boldsymbol{\sigma}(h)\\ \mathbf{q}_\alpha(h)\end{Bmatrix}, \quad \alpha = 1, \dots niv \tag{43}$$

must be unconditionally stable and consistent with the plastic part of the constitutive equations (25).

The constitutive equations (25) may admit closed form solutions for particular forms of $\mathbf{T}(\boldsymbol{\sigma}, \mathbf{q}_1, \dots, \mathbf{q}_{niv})$ and $\mathbf{f}_\alpha(\boldsymbol{\sigma}, \mathbf{q}_1, \dots, \mathbf{q}_{niv})$ appearing in (25). This introduces the possibility of using the closed form solutions to (25) as the algorithm $\mathbf{F}^{pl}(h)$ and is the approach used here. It should be emphasized, however, that the plastic relaxation equations (25) will not admit closed form solutions in general. That closed form solutions may be found in the present case results from the simplicity of the assumed structure of the constitutive mappings. In general, as in the case of $\mathbf{F}^{el}(h)$ given above, numerical solution schemes for (25) will have to be resorted to with the usual considerations for consistency, numerical stability and incremental objectivity.

Four examples of the constitutive mappings $\mathbf{T}(\boldsymbol{\sigma}, \mathbf{q}_\alpha)$ and $\mathbf{f}_\alpha(\boldsymbol{\sigma}, \mathbf{q}_\alpha)$ appearing in (25) are given according to the discussion in Section 2.2. These examples include perfect viscoplasticity and perfect plasticity (limiting case of viscoplasticity, see Section 2.2.1), hardening viscoplasticity and hardening plasticity (see Section 2.2.2). Closed form solutions for (25) corresponding to these constitutive equations have been found in [15,16] for use in a different context and will be utilized here. These solutions are summarized as follows.

3.3.2.1. Perfect Viscoplasticity

Noting again that no internal variables are needed for this model, the algorithm (43) becomes

$$\mathbf{F}^{pl}(h)(\boldsymbol{\sigma}) = \boldsymbol{\sigma}(h). \tag{44}$$

Using (20), the relaxation equations (25) take the form

$$\partial\boldsymbol{\sigma}/\partial t = -\mathbf{a} : \mathbf{T}(\boldsymbol{\sigma}) = -\mathbf{a} : \frac{\boldsymbol{\sigma} - \mathbf{P}_C\boldsymbol{\sigma}}{\eta} \tag{45}$$

where it is recalled from Section 2.2.1 that C denotes the convex elastic domain in stress space, $\mathbf{P}_C$ denotes the closest point mapping relative to C and the parameter η is the viscosity of the material. Eq. (45) represents a system of ordinary differential equations whose solution is

$$\boldsymbol{\sigma}(t) = \begin{cases}\boldsymbol{\sigma}_o & \textit{if } \boldsymbol{\sigma}_o \in C\\ \exp(-\mathbf{a}\, t/\eta) : \boldsymbol{\sigma}_o + [\mathbf{I} - \exp(-\mathbf{a}\, t/\eta)] : \mathbf{P}_C\boldsymbol{\sigma}_o & \textit{otherwise}\end{cases} \tag{46}$$

For the case of isochoric plasticity in which C is a cylinder oriented along the hydrostatic axis and for isotropic elasticity, eq. (46.b) simplifies to

$$\begin{aligned}\boldsymbol{\sigma}(t) &= e^{-t/\tau}\boldsymbol{\sigma}_o + (1 - e^{-t/\tau})\,\mathbf{P}_C\boldsymbol{\sigma}_o \\ &= p_o\mathbf{I} + e^{-t/\tau}\mathbf{s}_o + (1 - e^{-t/\tau})\,\mathbf{P}_C\mathbf{s}_o\end{aligned} \tag{47}$$

where $p_o = \boldsymbol{\sigma}_o\!:\!\mathbf{I}$ is the initial hydrostatic pressure, $\mathbf{s}_o$ is the deviatoric part of $\boldsymbol{\sigma}_o$ and $\tau = \eta/G$ is the relaxation time of the process, given in terms of the shear modulus of the material G.

For the von Mises yield criterion, the elastic domain C is the set $\{\boldsymbol{\sigma} \in S$ *such that* $J_2 \leqslant k^2\}$, where k is the shear yield stress, $J_2 = 1/2\,\mathbf{s}\!:\!\mathbf{s}$ and $\mathbf{s}$ is the deviatoric part of $\boldsymbol{\sigma}$. In this case, eq. (47) reduces to

$$\boldsymbol{\sigma}(t) = p_o\mathbf{I} + e^{-t/\tau}\,\mathbf{s}_o + (1 - e^{-t/\tau})\,\frac{k}{r_o}\,\mathbf{s}_o \tag{48}$$

where $r_o = (1/2\,\mathbf{s}_o\!:\!\mathbf{s}_o)^{\frac{1}{2}}$.

As noted above, these closed form solutions can be used for the $\mathbf{F}^{pl}(h)$ algorithm. While this algorithm is obviously consistent with (25) specialized for the given constitutive equations, the stability of the algorithm is not automatic. A general discussion of the requirements for unconditional stability of $\mathbf{F}^{pl}(h)$ can be found in [15,16] where it is also demonstrated that the solutions presented above satisfy such requirements.

Finally, the product algorithm (31) consists of first integrating the elastic constitutive equations, with time step h, ignoring the plasticity of the material. The stresses resulting from this operation are then allowed to relax according to (46) for a period of time h, Fig. 2. Clearly, the stresses resulting from the application of the elastic algorithm that lie inside the elastic region are unaffected by this relaxation process. The unconditional stability of the product algorithm follows from the unconditional stability of the component algorithms $\mathbf{F}^{el}(h)$ and $\mathbf{F}^{pl}(h)$.

3.3.2.2. Perfect Plasticity

As discussed in Section 2.2.1, perfect plasticity is considered as the limiting case of viscoplasticity as the viscosity η tends to zero or as an infinite period of time is allowed to elapse permitting the relaxation of the stress towards the elastic domain C. Taking this limit on the viscoplastic algorithm (44), the detailed form of which is given by (46), an algorithm for the case of perfect plasticity can be expressed as

$$\mathbf{F}^{pl}(h)(\boldsymbol{\sigma}) = \boldsymbol{\sigma}(\infty) = \mathbf{P}_C\,\boldsymbol{\sigma} \tag{49}$$

where $\mathbf{P}_C\boldsymbol{\sigma}$ again denotes the closest point projection of $\boldsymbol{\sigma}$ onto the elastic domain C. If

$\sigma \in C$ then $\mathbf{P}_C \sigma = \sigma$ and the stresses are unaffected by the plastic algorithm. It is noted that (49) is independent of the time step size h, reflecting the rate-independent character of this algorithm.

Applying this limiting condition to (48), an algorithm for perfect plasticity with the von Mises yield condition results and is given by

$$\mathbf{F}^{pl}(h)(\sigma) = \sigma(\infty) = \mathbf{P}_C \sigma = \begin{cases} \sigma & \text{if } r \leqslant k \\ p_0 \mathbf{I} + \dfrac{k}{r_0} \mathbf{s}_0 & \text{otherwise} \end{cases} \tag{50}$$

A more rigorous mathematical treatment of the viscoplastic approximation to inviscid plasticity can be found in [26].

The closest point mapping algorithm (49) may be viewed as a "return mapping" algorithm, other examples are discussed in [27,28,29,30]. Certainly, the closest point mapping does not exhaust all the possible choices of return mapping that can be used to project stresses back to the elastic domain. If consistent numerical schemes are introduced for the integration of the plastic constitutive equations, rather than the closed form solution adopted above, then these algorithms will result in various return mappings of the stress. A set of conditions on the return mapping has been presented in [26] that guarantees the consistency and numerical stability of the resulting plastic algorithm. In particular, it is demonstrated in [26] that the algorithm (50) satisfies the conditions for unconditional stability.

Finally, for the case of perfect plasticity, the product algorithm (31) consists of integrating the elastic constitutive equations with time step h, ignoring the plasticity of the material. The stresses resulting from this operation are then projected onto the closest point of the elastic domain C, Fig. 2. The unconditional stability of the product algorithm again follows from the unconditional stability of the component algorithms $\mathbf{F}^{el}(h)$ and $\mathbf{F}^{pl}(h)$.

3.3.2.3. Hardening Viscoplasticity

Using (21) and (22), the relaxation equations (25) take the form

$$\begin{aligned} \partial\sigma/\partial t &= -\mathbf{a} : \mathbf{T}(\sigma, \mathbf{q}) = -\mathbf{a} : \frac{\sigma - \mathbf{P}_{C(\mathbf{q})}\sigma}{\eta} \\ \overset{\circ}{\mathbf{q}}_\alpha &= \mathbf{f}_\alpha(\sigma, \mathbf{q}), \qquad \alpha = 1, \ldots, niv \end{aligned} \tag{51}$$

where $\mathbf{q}$ represents the set of spatial internal variables $\{\mathbf{q}_\alpha\}$, $\alpha = 1, \ldots, niv$.

For the case of isotropic hardening we take $niv = 1$ and identify $\mathbf{q}_1 = k$. Noting (3), it follows that

$$\overset{\circ}{k} = \partial k/\partial t + \partial k/\partial \mathbf{x} \cdot \mathbf{v} + k\, tr(\mathbf{d}). \tag{52}$$

Assuming a von Mises yield criterion with isotropic bilinear hardening and isotropic elasticity, (51) reduces to

$$\begin{aligned} \partial\boldsymbol{\sigma}/\partial t &= -\,2G\,\mathbf{d}^p = \frac{-\,G<\sqrt{J_2}-k>}{\eta}\,\frac{\mathbf{s}}{\sqrt{J_2}} \\ \partial k/\partial t &= 2H\,(\frac{1}{2}\,\mathbf{d}^p{:}\mathbf{d}^p)^{1/2} = H\,\frac{<\sqrt{J_2}-k>}{\eta} \end{aligned} \tag{53}$$

where H denotes the shear plastic modulus. Note that the last two terms on the right hand side of (52) have been neglected. The solution of (53) is found to be [15,16]

$$\begin{aligned} &\boldsymbol{\sigma}(t) = \boldsymbol{\sigma}_o \quad , \quad k(t) = k_o \quad , \quad if\ r_o \leqslant k_o \\ &\left.\begin{aligned} \boldsymbol{\sigma}(t) &= \boldsymbol{\sigma}_o - \frac{\tau}{\tau_s}(r_o - k_o)(1 - e^{-t/\tau})\,\frac{\mathbf{s}_o}{r_o} \\ k(t) &= k_o + \frac{\tau}{\tau_q}(r_o - k_o)(1 - e^{-t/\tau}) \end{aligned}\right\} \quad otherwise \end{aligned} \tag{54}$$

where

$$\tau_s = \frac{\eta}{G} \quad ; \quad \tau_q = \frac{\eta}{H} \quad ; \quad \tau = \frac{\tau_s \tau_q}{\tau_s + \tau_q} \tag{55}$$

are relaxation times for the process.

It is seen from (54) that during a relaxation process corresponding to initial stresses outside the elastic domain, the stresses steadily approach the elastic domain, which at the same time expands towards the stress point. As in the case of perfect viscoplasticity, the closed form solution (54) can be utilized to define the plastic algorithm (43). Requirements for the unconditional stability of (54) are considered in [15] where a similar algorithm is presented for the case of kinematic hardening.

3.3.2.4. Hardening Plasticity.

As in the case of perfect plasticity, plastic algorithms for the hardening case can be obtained as the limiting case of (43) as the viscosity η tends to zero or as an infinite length of time is allowed for the relaxation of the stress and internal variables and is expressed by

$$\mathbf{F}^{pl}(h)\begin{Bmatrix}\boldsymbol{\sigma}\\ \mathbf{q}_\alpha\end{Bmatrix} = \begin{Bmatrix}\boldsymbol{\sigma}(\infty)\\ \mathbf{q}_\alpha(\infty)\end{Bmatrix}, \quad \alpha = 1,\ldots,niv \tag{56}$$

For the case of bilinear isotropic hardening and a von Mises yield criterion, the asymptotic values in (56) can be obtained from (54) as

$$
\begin{aligned}
&\sigma(\infty) = \sigma_o \quad , \quad k(\infty) = k_o \quad \text{if } r_o \leqslant k_o \\
&\sigma(\infty) = \sigma_o - \frac{G}{G+H}(r_o - k_o)\,\frac{\mathbf{s}_o}{r_o} \\
&k(\infty) = k_o + \frac{H}{G+H}(r_o - k_o) \qquad \textit{otherwise}
\end{aligned}
\tag{57}
$$

Note that these limiting values are independent of η and the time step size h.

Eq. (57) yields a suitable "return mapping" for the isotropic hardening rule. It is seen from (57) that the stress point and the yield surface meet at some intermediate point on the segment joining their initial values, the distances from these being proportional to G and H, respectively. A similar geometric interpretation can be derived for the return mapping corresponding to the kinematic hardening rule [15]. Note that the perfectly plastic case is recovered by setting $H = 0$.

Finally, the unconditional stability of the plastic algorithm induced by this return mapping follows from that of the corresponding viscoplastic case. Consequently, the unconditional stability of the product algorithm (31) follows from the unconditional stability of the component algorithms $\mathbf{F}^{el}(h)$ and $\mathbf{F}^{pl}(h)$.

4. Global Algorithms for the Finite Deformation Dynamic Problem

4.1. Introduction

As noted in Section 1, the development of global algorithms for the solution of the boundary value problem of linear momentum balance is outside the scope of the present paper. However, the global solution algorithm and the algorithm for the integration of the rate constitutive equations will be interdependent and cannot be entirely separated in any reasonably complete discussion of either algorithm. Accordingly, a brief description of global algorithms is presented, including "implicit" algorithms which employ an elastoplastic (or elasto-viscoplastic) tangent modulus tensor and a product algorithm based on an operator split of the momentum balance equation. It is noted that both these global algorithms suffer from computational disadvantages that make their use very costly in general. An alternative global algorithm is therefore proposed.

4.2. Boundary Value Problem of Linear Momentum Balance

The boundary value problem of linear momentum balance for elastoplastic or elasto-viscoplastic materials introduced in Section 2 is summarized as

$$
\begin{aligned}
\dot{\boldsymbol{\phi}}_t &= \mathbf{v} \circ \boldsymbol{\phi}_t \\
\rho\,\dot{\mathbf{v}} &= \nabla \cdot \boldsymbol{\sigma} + \rho\,\mathbf{b} \\
\overset{\circ}{\boldsymbol{\sigma}} &= \mathbf{a} : (\mathbf{d} - \mathbf{T}(\boldsymbol{\sigma}, \mathbf{q}_1, \ldots, \mathbf{q}_{niv})) \\
\overset{\circ}{\mathbf{q}}_\alpha &= \mathbf{f}_\alpha(\boldsymbol{\sigma}, \mathbf{q}_1, \ldots, \mathbf{q}_{niv}) \quad \alpha = 1, \ldots, niv
\end{aligned}
\tag{58}
$$

A variety of techniques has been proposed for the solution of (58) (although many of these have been based on the equivalent rate of momentum balance problem derived from time differentiation of (58.b) together with appropriate traction and kinematic rate boundary conditions). Implicit methods which employ an elastoplastic "tangent" modulus, e.g. [22,24,25], suffer from numerical difficulties associated with enforcing the consistency condition of plasticity which requires that the stress trajectory be confined to the elastic domain. Frequently, projection techniques have been introduced to restore consistency. Such methods also require elaborate schemes for making the transition from the elastic to the plastic regimes and frequently require truncating or discarding of time steps. Although these methods are potentially quite accurate, they can be very costly in practice.

The limitations of the tangent modulus methods motivated a search for alternative methods of solution. One such alternative method, originally proposed by Mendelson [30] for the case of infinitesimal plasticity, employs the concept of a "return mapping" algorithm which automatically ensures satisfaction of the plastic consistency condition. The accuracy of this method has also been considered for a limited class of material models [27,28,29].

In order to be convergent, a numerical solution scheme must satisfy the requirements of consistency and numerical stability. A formal study of the consistency and numerical stability properties of global solution schemes arising from the use of return mapping algorithms has recently been considered within the framework of operator split methods [15,16,26]. It is noted in [16] that the field equations (58) exhibit an additive decomposition into an "elastic" part (which defines an elastodynamic boundary value problem in which only the motion and stress tensor are involved) and a "plastic" part (which leaves the configuration unchanged and defines a pointwise relaxation process for the stress tensor and internal variables). This suggests using the product formula techniques discussed in Section 3.2 to construct a solution algorithm for (58).

In the present context, a product algorithm relative to the elastoplastic additive decomposition of the equations of motion takes the following meaning [16]. Consider two algorithms $\mathbf{G}^{el}(h)$ and $\mathbf{G}^{pl}(h)$ which are consistent in the sense of (27) with the "elastic" and "plastic" parts of (58) respectively and which are unconditionally stable in the sense of (28). Then an unconditionally stable algorithm $\mathbf{G}(h)$ consistent with the full equations of motion (58) can be obtained by means of the general product formula (30) such that

$$\mathbf{G}(h) = \mathbf{G}^{pl}(h)\,\mathbf{G}^{el}(h) \tag{59}$$

The product formula (59) simply states that a solution algorithm for the elastoplastic problem can be obtained by solving for each time step an elastic dynamic problem first, and then applying to the solution vector so obtained a plastic algorithm operating on the stresses and internal variables bringing in the effect of the plastic constitutive equations. It is interesting to note that all the boundary value aspects of the elastoplastic dynamic problem are included in the "elastic" part of (58) and are taken care of by the elastic algorithm $\mathbf{G}^{el}(h)$ [16].

In practice, the above equations are solved by means of some spatial discretization technique such as the finite element method. In this case, the "plastic" part of the equations of motion will correspond to a set of relaxation equations expressed at the integration points within the elements and the plastic algorithm $\mathbf{G}^{pl}(h)$ is accordingly applied integration point by integration point. The construction of the global algorithm given by (59) is discussed in detail in [16].

Although the unconditionally stable global product algorithm described above is consistent with the field equations it is observed in [16] that the accuracy of the global product algorithm deteriorates as the size of the time step is increased. The effectiveness of the operator split method depends strongly on the error introduced by the splitting. Experience in a number of areas of application indicate that the splitting error dominates beyond certain critical time step sizes [14,15,16]. For some problems these critical time step sizes are small enough to eliminate the possible benefits of the method.

The fully implicit methods employing the elastoplastic tangent modulus are potentially more accurate than the global product algorithm described above but suffer from the difficulties also noted above. In this paper an implicit global solution scheme based on the elastoplastic tangent modulus is proposed in combination with a product algorithm applied to the integration of the constitutive equations. It is demonstrated below that such a scheme eliminates the difficulties associated with the implicit methods and results in an accurate and efficient solution procedure.

4.3. Alternative Implicit Global Algorithm

The global algorithm is an iterative scheme based upon the consistent linearization of a weak form of the boundary value problem of linear momentum balance (58). The construction of the weak form as well as the mathematical ideas necessary for the consistent linearization of the weak form will not be discussed in detail here. Similar notions have been considered in [16,20]. The construction of this implicit global algorithm entails the following steps:

(i) Spatially Discretized Weak Form

A weak form of (58) is expressed by

$$\int_{\phi_t(B)} [\rho\,(\dot{\mathbf{v}} - \mathbf{b}) \cdot \boldsymbol{\eta} + \boldsymbol{\sigma} : \nabla \boldsymbol{\eta}]\, dv = \int_{\partial_\sigma \phi_t(B)} \bar{\mathbf{t}} \cdot \boldsymbol{\eta}\, da \tag{60}$$

for all weighting functions $\boldsymbol{\eta}$ which satisfy the homogeneous boundary conditions on $\partial_u \boldsymbol{\phi}_t(B)$. Spatial discretization of (60) can be accomplished using the finite element method in which a set of global finite element interpolation functions is introduced for the nodal values of the motion $\boldsymbol{\phi}_t$ and the weighting functions $\boldsymbol{\eta}$. In the present "displacement" method the stress is not independently interpolated but is thought of as being a function of the motion. In this case the spatially discretized weak form (60) can be expressed as

$$\mathbf{M} \cdot \dot{\mathbf{v}} + \mathbf{P}(\boldsymbol{\sigma}, t) = \mathbf{F}(t) \tag{61}$$

where $\mathbf{M}$ is the mass matrix, $\mathbf{v}$ is the vector of nodal velocities, $\mathbf{P}(\boldsymbol{\sigma}, t)$ is the "internal force" vector and $\mathbf{F}(t)$ is the global force vector.

(ii) Temporal Integration of the Weak Form

The spatially discretized weak form (61) can be numerically integrated in time by the application of an algorithm such as the implicit Newmark algorithm defined by

$$\mathbf{M} \cdot \dot{\mathbf{v}}_{n+1} + \mathbf{P}_{n+1}(\boldsymbol{\sigma}_{n+1}) = \mathbf{F}_{n+1} \tag{62}$$

$$\boldsymbol{\phi}_{n+1} = \boldsymbol{\phi}_n + h \mathbf{v}_n + h^2[(\frac{1}{2} - \beta)\dot{\mathbf{v}}_n + \beta \dot{\mathbf{v}}_{n+1}] \tag{63}$$

$$\mathbf{v}_{n+1} = \mathbf{v}_n + h[(1-\gamma)\dot{\mathbf{v}}_n + \gamma \dot{\mathbf{v}}_{n+1}] \tag{64}$$

where subscripts n and $n+1$ denote variables evaluated at the nth and $n+1$th time steps, $h = t_{n+1} - t_n$ is the time step size and β and γ are the Newmark parameters. Substituting (63) and (64) into (62) results in

$$G(\boldsymbol{\phi}_{n+1}) \equiv \frac{1}{\beta h^2}\mathbf{M} \cdot \boldsymbol{\phi}_{n+1} + \mathbf{P}_{n+1}(\boldsymbol{\sigma}_{n+1}) - \hat{\mathbf{P}}_{n+1} = 0 \tag{65}$$

where $\hat{\mathbf{P}}_{n+1} = \mathbf{F}_{n+1} - \mathbf{M} \cdot [(1 - \frac{1}{2\beta})\dot{\mathbf{v}}_n - \frac{1}{\beta h}\mathbf{v}_n - \frac{1}{\beta h^2}\boldsymbol{\phi}_n]$. For this formulation $\beta \neq 0$.

(iii) Linearization

Formally, it is found that a consistent linearization procedure may be based on Taylor's formula for C^1 functions [9,31]. Without entering into mathematical detail, the linearization of (65) about the motion $\boldsymbol{\phi}_{n+1}$ can be expressed as

$$L[G(\boldsymbol{\phi}_{n+1})] = G(\boldsymbol{\phi}_{n+1}) + \mathbf{D}G(\boldsymbol{\phi}_{n+1}) \cdot \mathbf{u}_{n+1} = 0 \tag{66}$$

where

$$\mathbf{D}G(\boldsymbol{\phi}_{n+1}) \cdot \mathbf{u}_{n+1} = \frac{1}{\beta h^2}\mathbf{M} \cdot \mathbf{u}_{n+1} + \mathbf{D}\mathbf{P}_{n+1} \cdot \mathbf{u}_{n+1}. \tag{67}$$

is the directional derivative of $G(\boldsymbol{\phi}_{n+1})$ in the direction of the incremental motion $\mathbf{u}_{n+1}$ [16]. Similarly, in (67) $\mathbf{DP}_{n+1} \cdot \mathbf{u}_{n+1}$ is the directional derivative of the internal force vector. This last directional derivative involves finding the directional derivative of the spatial stress tensor. This can be accomplished by using results from differential geometry. The consistent approximation of a certain derivative appearing in the development allows the introduction of the rate constitutive equations for the stress given by (58.c). Details may be found in [16].

Combining the above concepts with the product algorithm (31) for the integration of the rate constitutive equations, an iterative Newton-Raphson solution scheme can be expressed as

$$
\begin{aligned}
&(i) && \mathbf{D}G(\boldsymbol{\phi}^{i}_{n+1}) \cdot \mathbf{u}^{i}_{n+1} \equiv \mathbf{K}^{i}_{n+1} \cdot \mathbf{u}^{i}_{n+1} \\
&(ii) && \mathbf{u}^{i}_{n+1} = -(\mathbf{K}^{i}_{n+1})^{-1} \cdot G(\boldsymbol{\phi}^{i}_{n+1}) \\
&(iii) && \boldsymbol{\phi}^{i+1}_{n+1} = \boldsymbol{\phi}^{i}_{n+1} + \mathbf{u}^{i}_{n+1} \\
&(iv) && \begin{Bmatrix} \boldsymbol{\sigma} \\ \mathbf{q}_{\alpha} \end{Bmatrix}^{i+1}_{n+1} = \mathbf{F}^{pl}(h)\, \mathbf{F}^{el}(h) \begin{Bmatrix} \boldsymbol{\sigma} \\ \mathbf{q}_{\alpha} \end{Bmatrix}_{n} \\
&(v) && i \leftarrow i+1, \;\; go\ to\ (i).
\end{aligned}
\tag{68}
$$

where the superscript i is the iteration counter within the time step $h = t_{n+1} - t_n$. The quantity with no superscript appearing on the right hand side of (iv) implies that the converged values at the indicated time are to be used.

The solution procedure is illustrated by means of an example in Fig. 3. The problem concerns an elastoplastic material with isotropic hardening subjected to a cycle of uniaxial tension while in a state of plane strain. Fig. 3, which depicts axial stress versus axial stretch, illustrates two solutions. One of these corresponds to the global product algorithm (59) reported in [16] and discussed in Section 4.2 and the other corresponds to a solution obtained from the algorithm given by (68). The solution obtained by use of (59) employed 400 time steps. In contrast, the solution obtained by use of (68) employed a total of 4 time steps. With reference to the algorithm (68), the following comments apply:

(a) In the first iteration of each time step ($i = 1$) the "tangent modulus matrix" $\mathbf{K}^1$ is assumed to be only elastic and the product algorithm (iv) employs only the elastic algorithm $\mathbf{F}^{el}(h)$.

(b) If the resulting stress lies inside the elastic domain the iterative procedure progresses by ignoring the plasticity of the material (although in each subsequent iteration the stresses are always checked to ensure that their trajectory lies inside the elastic domain). However, if the stress lies outside the elastic domain the tangent modulus matrix $\mathbf{K}^i$ is modified to include the plastic constitutive equations and the full product algorithm (iv) is employed.

In this way the transition from elastic to plastic loading is handled automatically. Fig. 3 shows the results of step (iv) in the last iteration of each of the four time steps. The points marked a and b correspond to $\mathbf{F}^{el}(h)\begin{Bmatrix}\boldsymbol{\sigma}\\ \mathbf{q}_\alpha\end{Bmatrix}$ and $\mathbf{F}^{pl}(h)\,\mathbf{F}^{el}(h)\begin{Bmatrix}\boldsymbol{\sigma}\\ \mathbf{q}_\alpha\end{Bmatrix}$ respectively. It is evident that the algorithm (68) employing 4 time steps is close to the solution given by (59) which employed 400 time steps. The solution obtained from from (59) with 4 time steps is extremely inaccurate, with streses in error by almost 50% (this solution is not shown in Fig. 3).

5. Improving Accuracy by Time Step Refinement

The operator split of (23) into (24) and (25) will introduce an error into the associated product formula (31) which is step (iv) in (68). For viscoplasticity (plasticity) the spatial stress tensor plays a dominant role in the definition of the tangent modulus matrix $\mathbf{K}$ and it is thus important for the convergence rate of the Newton-Raphson scheme (68) that this tensor be evaluated as accurately as possible from the integration of the rate constitutive equations. This suggests that by improving the accuracy of (31) the overall scheme will enjoy an improved convergence rate without changing the global time size. This may be accomplished by modifying (31) to the following form

$$\mathbf{F}(h) = \prod_{i=1}^{N} \mathbf{F}_i^{pl}\left(\frac{h}{N}\right) \mathbf{F}_i^{el}\left(\frac{h}{N}\right) \tag{69}$$

The algorithm defined by (69) involves subdividing the time step into N parts and applying the product algorithm N times. The algorithms $\mathbf{F}_i^{el}$ and $\mathbf{F}_i^{pl}$ have the form described in Sections 3.3.1 and 3.3.2 respectively.

This algorithm will satisfy the requirements of consistency in the sense of (27) and stability in the sense of (28). However, the requirement of incremental objectivity places a restriction on the interpretation of $\mathbf{F}^{el}(\frac{h}{N})$. Recalling equations (40) - (42), which are the detailed form of $\mathbf{F}^{el}(h)$, it may be shown that incremental objectivity is satisfied in (69) only if $\mathbf{d}_{n+\alpha}$ appearing in (42) is replaced by $\frac{\mathbf{d}_{n+\alpha}}{N}$. Thus the deformation gradient over the interval h is subdivided rather than the deformation itself. The resulting algorithm appears to display excellent accuracy for N in the range of 2 to 5 for numerical examples which have been considered.

As an example, the cycle of uniaxial loading for the plane strain problem discussed above is again considered. Fig. 4 shows two plots of stress versus axial stretch. The solution obtained from the global product algorithm (59) in 400 time steps is again shown. The other curve in Fig. 4 shows the results for the algorithm (68) modified by using (69) for step (iv). As before, four time steps are taken globally but N in (69) is selected as 5. The curve again shows the stress plotted for the solution at the last iteration in each of the four time steps. The increase in accuracy is evident by comparing Figs. 3 and 4.

A further example of the accuracy of the algorithm given by (68) - (69) compared to the global product algorithm (59) is shown in Fig. 5 which depicts the stress distribution in an infinitely long internally pressurized thick walled cylinder. The material is elastoplastic with isotropic hardening and a von Mises yield criterion. The tube was discretized by means of plane strain quadrilateral elements with 16 elements across the thickness. Fig. 5 depicts the stress components in the tube for an internal pressure corresponding to a plastification of 75% of the wall thickness. Five curves for each stress component are plotted. The curves 1 - 4 correspond to the global product algorithm (59) and were obtained with 2,4,8 and 100 time steps respectively. These curve illustrate the convergence of this algorithm. However, the curve denoted a in Fig. 5 corresponds, for each stress component, to the solution from the algorithm (68) - (69) with 2,4 and 8 global time steps. The value of N in (69) was taken as 2. These solutions are coincident and appear to be correct by comparison with the global product algorithm solutions. The accuracy of the present algorithm with 2 global time steps exceeds the accuracy of the global product algorithm with 100 time steps. Solutions for this problem with $N \geqslant 2$ did not result in a marked improvement of the convergence rate of the global algorithm although for problems with greater stress gradients this conclusion may not apply.

Acknowledgements

We would like to acknowledge the continued interest and encouragement of Dr. G.L. Goudreau of the Lawrence Livermore National Laboratory and Dr. T. Khalil of General Motors Research Laboratories. Support for this work from these agencies is also gratefully acknowledged.

References

1. B.D. Coleman and M.E. Gurtin, "Thermodynamics with Internal State Variables," *J. Chem. Phys. 47,* 597-613 (1967).

2. J. Lubliner, "On the Thermodynamic Foundations of Non-Linear Solid Mechanics," *Int. J. Non-linear Mechanics 7,* 237-254 (1972).

3. J. Lubliner, "On the Structure of the Rate Equations of Materials with Internal Variables," *Acta Mech. 17,* 109-119 (1973).

4. J.Mandel, "Thermodynamics and Plasticity," in J.J. Delgado Domingos, M.N.R. Nina and J.H. Whitelaw (editors), **Foundations of Continuum Thermodynamics,** 283-304, John Wiley and Sons, 1973.

5. C. Truesdell, "The Simplest Rate Theory of Pure Elasticity," *Comm. Pure Appl. Math., 8,* 123-132, 1955.

6. J.G. Oldroyd, "On the Formulation of Rheological Equations of State," *Proc. Roy. Soc., A200,* 523-541, 1950.

7. B.A. Cotter and R.S. Rivlin, "Tensors Associated with Time-Dependent Stress," *Quart. Appl. Math., 13,* 177-182, 1955.

8. D. Durban and M. Baruch, "Incremental Behavior of an Elasto-Plastic Continuum," TAE Report No. 193, Dept. of Aeronautical Eng., Israel Institute of Technology, Haifa, Israel, Feb. 1975.

9. J.E. Marsden and T.J.R. Hughes, "Topics in Mathematical Foundations of Elasticity," in R.J. Knops (Ed.), **Nonlinear Analysis and Mechanics,** Heriot-Watt Symposium, Vol. II, Pitman Publishing Co., 1978.

10. E.H. Lee and D.T. Liu, "Finite Strain Elastic-Plastic Theory Particularly for Plane Wave Analysis," *J. Appl. Phys., 38,* 19-27, (1967).

11. S. Nemat-Nasser, "Decomposition of Strain Measures and Their Rates in Finite Deformation Elastoplasticity," *Int. J. Solids Struct., 15,* 155-166 (1979).

12. A.E. Green and P.M. Naghdi, "Some Remarks on Elastic-Plastic Deformation at Finite Strain," *Int. J. Engng. Sci., 9,* 1219-1229 (1971).

13. T.J.R. Hughes, I. Levit and J. Winget, "Unconditionally Stable Element-by-Element Implicit Algorithms for Heat Conduction Analysis", *J. Engng. Mechs. Div. of ASCE,* (to appear).

14. M. Ortiz, P.M. Pinsky and R.L. Taylor, "Unconditionally Stable Element-by-Element Algorithms For Dynamic Problems," *Computer Methods in Applied Mechanics and Engineering,* (to appear).

15. M. Ortiz, P.M. Pinsky and R.L. Taylor, "Operator Split Methods for the Numerical Solution of the Elastoplastic Dynamic Problem," *Computer Methods in Applied Mechanics and Engineering,* (to appear).

16. P.M. Pinsky, M. Ortiz and R.L. Taylor, "Operator Split Methods in the Numerical Solution of the Finite Deformation Elastoplastic Dynamic Problem," Report No. UCB/SESM-82/03, Department of Civil Engineering, University of California, Berkeley, California, May, 1982.

17. G.W. Gear, **Numerical Initial Value Problems in Ordinary Differential Equations**, Prentice-Hall, 1971.

18. T.J.R. Hughes and J. Winget, "Finite Rotation Effects in Numerical Integration of Rate Constitutive Equations Arising in Large-Deformation Analysis," *Int. J. Num. Meth. Eng.*, *15*, No. 12, December 1980.

19. P.M. Pinsky, M. Ortiz and K.S. Pister, "Rate Constitutive Equations in Finite Deformation Analysis: Theoretical Aspects and Numerical Integration," *Computer Methods in Applied Mechanics and Engineering*, (to appear).

20. P.M. Pinsky, "A Numerical Formulation for the Finite Deformation Problem of Solids with Rate-Independent Constitutive Equations," Report No. UCB/SESM-81/07, Department of Civil Engineering, University of California, Berkeley, California, December, 1981.

21. J. Lubliner, "A Simple Theory of Plasticity," *Int. J. Solids Struct.*, *10*, 313-319 (1974).

22. R.M. McMeeking and J. R. Rice, "Finite Element Formulations for Problems of Large Elastic-Plastic Deformation," *Int. J. Solids Struct.*, *11*, 601 (1975).

23. B.D. Coleman and W. Noll, "The Thermodynamics of Elastic Materials with Heat Conduction and Viscosity," *Arch. Ration. Mech. Anal.*, *13*, 167-178, (1963).

24. R.D. Krieg, and S. W. Key, "Implementation of a Time-Independent Plasticity Theory into Structural Computer Programs," in: J. A. Stricklin and K. J. Saczalski (Eds.), *Constitutive Equations in Viscoplasticity: Computational and Engineering Aspects*, AMD, Vol. 20, ASME, 125 (1976).

25. J.O. Hallquist, "NIKE 2D: An Implicit, Finite-Deformation, Finite-Element Code for Analyzing the Static and Dynamic Response of Two-Dimensional Solids," Lawrence Livermore National Laboratory Report UCRL-52678, University of California, Livermore, March 3, 1979.

26. M. Ortiz and P.M. Pinsky, "Global Analysis Methods for the Solution of the Elastoplastic and Viscoplastic Dynamic Problems," Report No. UCB/SESM-81/08, Department of Civil Engineering, University of California, Berkeley, California, December, 1981.

27. R.D. Krieg and D.B. Krieg, "Accuracies of Numerical Solution Methods for the Elastic-Perfectly Plastic Model," *ASME J. Pressure Vessel Tech.*, **99**, 510-515, (1977).

28. H.L. Schreyer, R.F. Kulak and J.M. Kramer, "Accurate Numerical Solutions for Elastic-Plastic Models," *ASME J. Pressure Vessel Tech.*, **101**, 226-234, (1979).

29. J.M. Santiago, "On the Accuracy of Flow Rule Approximations Used in Structural and Solid Response Computer Programs," in: *Proceedings of the 1981 Army Numerical Analysis And Computers Conference*, ARO Report 81-3, (1981).

30. A. Mendelson, **Plasticity: Theory and Application**, McMillan, 1968.

31. T.J.R. Hughes and K.S. Pister, "Consistent Linearization in Mechanics of Solids and Structures," *Computers and Structures*, *8*, 391-397 (1978).

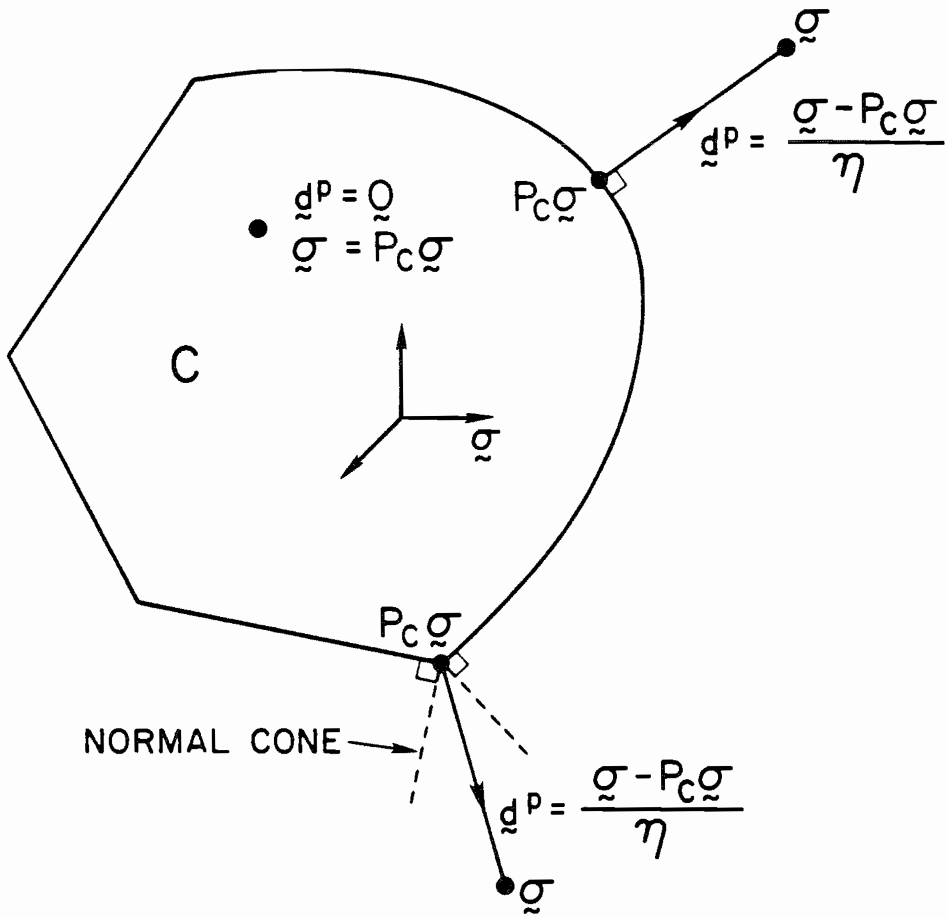

Fig. 1. Definition of viscoplastic constitutive mapping.

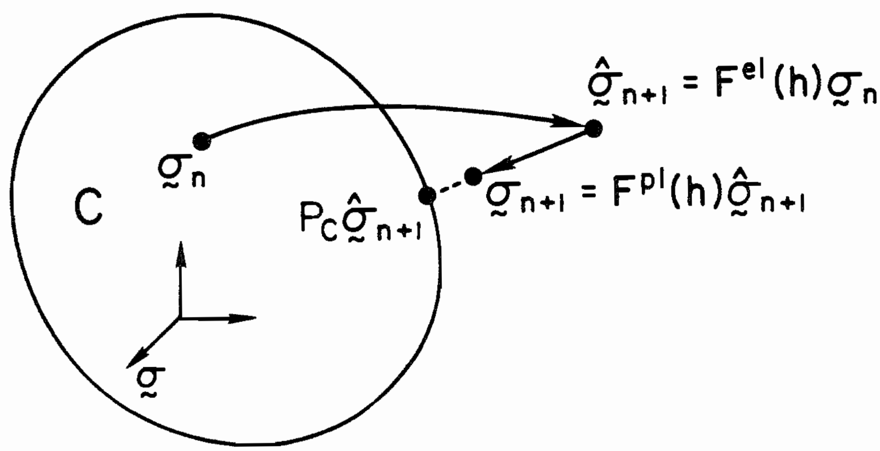

Fig. 2. Schematic representation of product algorithm.

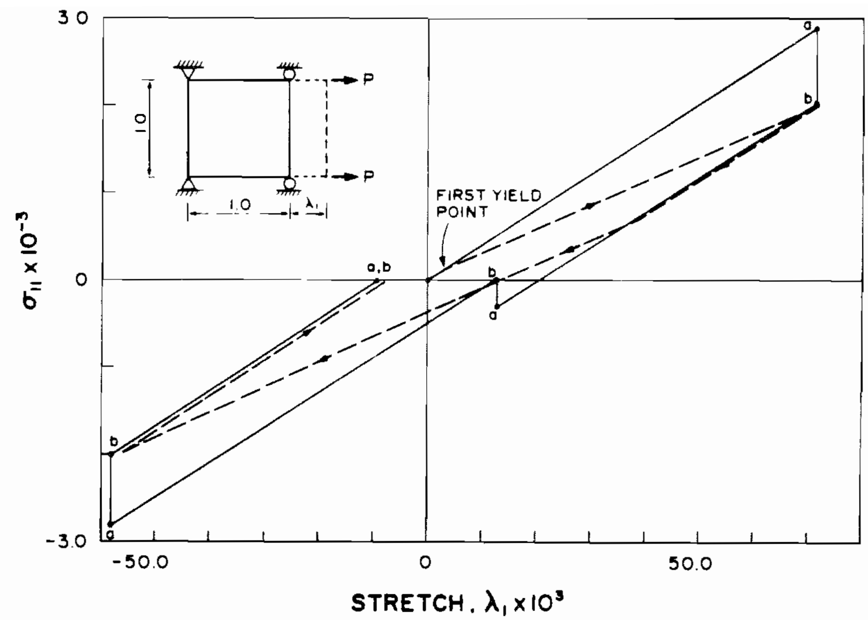

Fig. 3. Cycle of axial stress versus stretch for plane strain extension of an elastoplastic material with von Mises yield criterion and isotropic hardening. The dashed lines correspond to the global product algorithm (59) with 400 time steps. The solid lines correspond to the algorithm (68) with 4 time steps. Point *a* represents the "elastic" solution and point *b* the final solution for each time step.

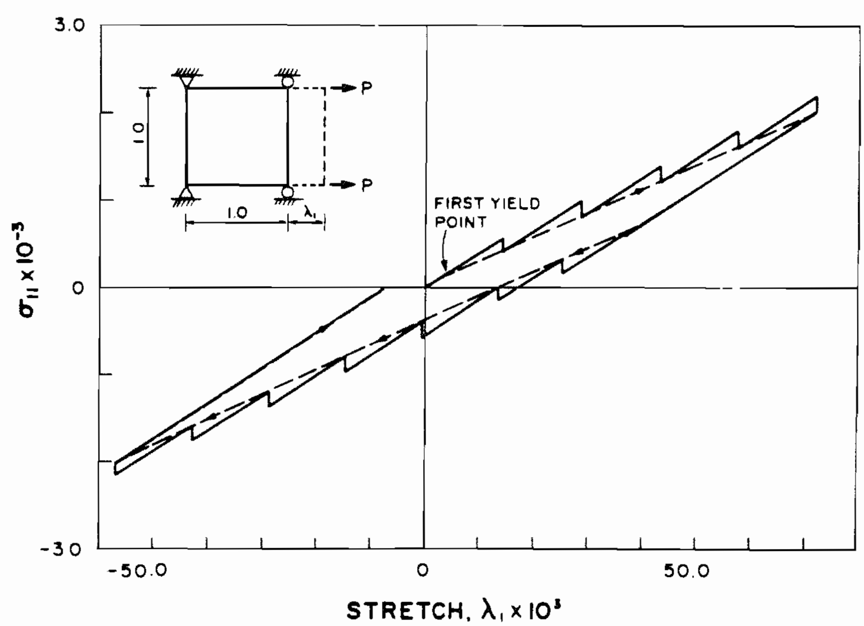

Fig. 4. Cycle of axial extension for material described in Fig. 3. The dashed lines correspond to the global product algorithm (59) with 400 time steps. The solid lines correspond to algorithm (68) - (69) with 4 time steps and $N = 5$ in (69).

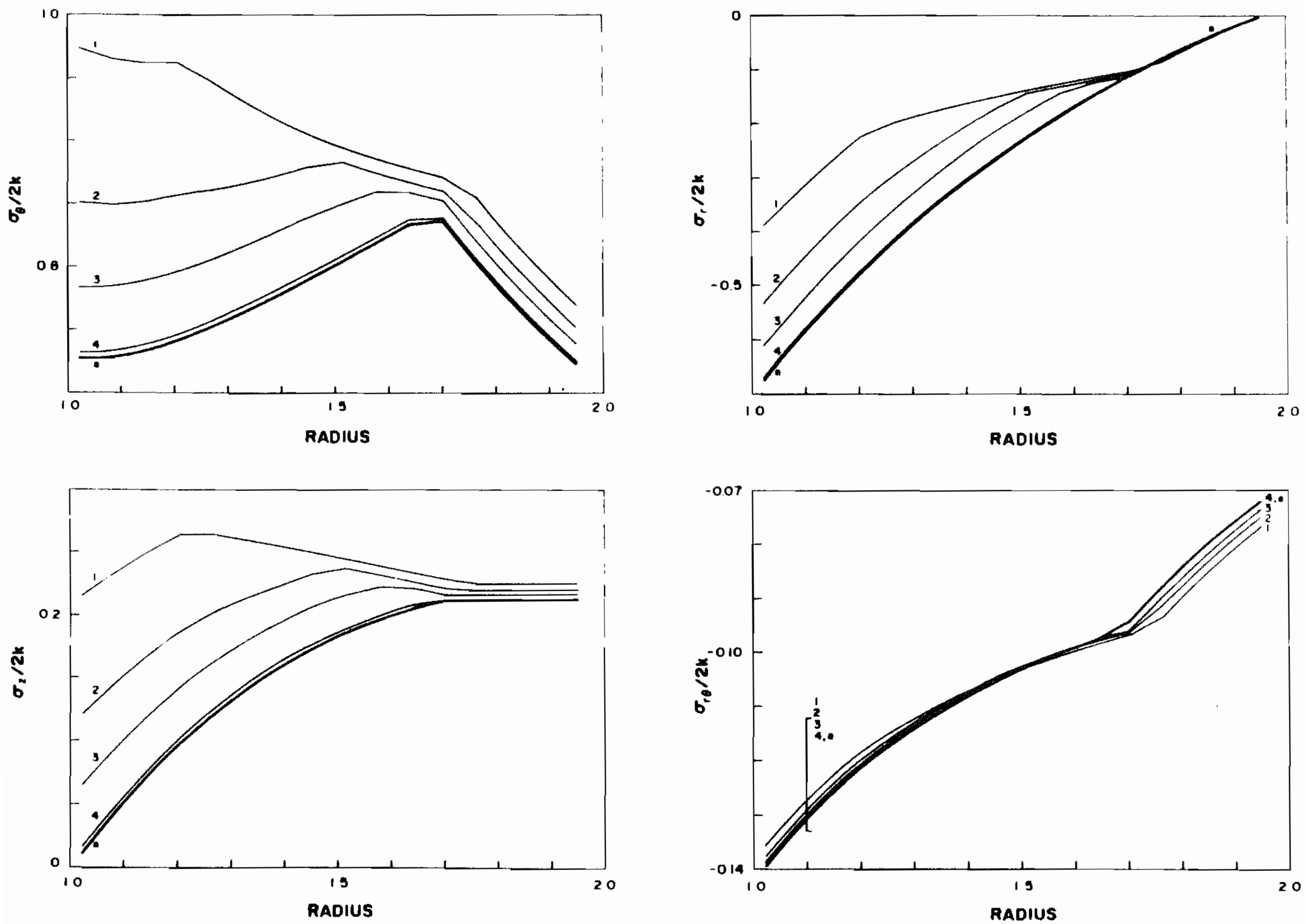

Fig. 5. Stress distribution through the wall thickness of an infinitely long internally pressurized thick walled cylinder. The material is isotropic hardening plasticity with a plastic hardening modulus which is 10% of the Young's modulus. Curves 1-4 correspond to algorithm (59) and were obtained with 2,4,8 and 100 time steps respectively. Curve *a* corresponds to the algorithm (68) - (69) with $N = 2$ and was obtained with 2,4 and 8 time steps (the solutions were coincident).